Neurotox Res (2010) 17:28–38
DOI 10.1007/s12640-009-9074-5

4-Hydroxy-2-Nonenal Induces Mitochondrial Dysfunction and Aberrant Axonal Outgrowth in Adult Sensory Neurons that Mimics Features of Diabetic Neuropathy

Eli Akude · Elena Zherebitskaya · Subir K. Roy Chowdhury · Kimberly Girling · Paul Fernyhough

Received: 17 February 2009 / Revised: 3 April 2009 / Accepted: 26 April 2009 / Published online: 26 June 2009

Abstract Modification of proteins by 4-hydroxy-2-nonenal (4-HNE) has been proposed to cause neurotoxicity in a number of neurodegenerative diseases, including distal axonopathy in diabetic sensory neuropathy. We tested the hypothesis that exposure of cultured adult rat sensory neurons to 4-HNE would result in the formation of amino acid adducts on mitochondrial proteins and that this process would be associated with impaired mitochondrial function and axonal regeneration. In addition, we compared 4-HNE-induced axon pathology with that exhibited by neurons isolated from diabetic rats. Cultured adult rat dorsal root ganglion (DRG) sensory neurons were incubated with varying concentrations of 4-HNE. Cell survival, axonal morphology, and level of axon outgrowth were assessed. In addition, video microscopy of live cells, western blot, and immunofluorescent staining were utilized to detect protein adduct formation by 4-HNE and to localize actively respiring mitochondria. 4-HNE induced formation of protein adducts on cytoskeletal and mitochondrial proteins, and impaired axon regeneration by approximately 50% at 3 μM while having no effect on neuronal survival. 4-HNE initiated formation of aberrant axonal structures and caused the accumulation of mitochondria in these dystrophic structures. Neurons treated with 4-HNE exhibited a distal loss of active mitochondria. Finally, the distal axonopathy and the associated aberrant axonal structures generated by 4-HNE treatment mimicked axon pathology observed in DRG sensory neurons isolated from diabetic rats and replicated aspects of neurodegeneration observed in human diabetic sensory neuropathy.

Keywords Amino acid adducts · Diabetes · DRG · Neuropathy · Chloromethyl-x-rosamine · Axonal dystrophy · Oxidative stress · Lipid peroxidation

Introduction

4-hydroxy-2-nonenal (4-HNE) is a highly reactive α,β-unsaturated aldehyde formed from the breakdown of polyunsaturated fatty acids in cholesterol esters, phospholipids, and triglycerides (Uchida 2003). It is a major product of lipid peroxidation and the pathway for its production and biotransformation has been well characterized (Uchida 2003; Carini et al. 2004; Petersen and Doorn 2004). 4-HNE exhibits a variety of biological activities including inhibition of protein and DNA synthesis (Sayre et al. 2006) and inactivation of enzymes (Isom et al. 2004). 4-HNE can form protein adducts with amino acid residues such as cysteine, histamine, and lysine due to its strong electrophilic properties (Uchida 2003; Isom et al. 2004). Moreover, the presence of these protein adducts can serve as biomarkers for the occurrence and extent of oxidative stress (Uchida 2003). Earlier studies have also demonstrated the ability of 4-HNE to act as a signaling molecule, which induces a variety of cellular processes (Awasthi

E. Akude · E. Zherebitskaya · S. K. Roy Chowdhury · K. Girling · P. Fernyhough (✉)
Division of Neurodegenerative Disorders, St Boniface Hospital Research Centre, R4046-351 Tache Ave, Winnipeg, MB R2H 2A6, Canada
e-mail: paulfernyhough@yahoo.com

E. Akude · P. Fernyhough
Department of Pharmacology & Therapeutics, University of Manitoba, Winnipeg, MB, Canada

et al. 2003; Forman et al. 2003). In addition, 4-HNE has been shown to inhibit neurite outgrowth, disrupt microtubules, and modify tubulin in Neuro 2A neuroblastoma cells (Neely et al. 1999; Kokubo et al. 2008), and it's cytotoxic and genotoxic effects have been demonstrated in cerebral endothelial cells (Karlhuber et al. 1997).

4-HNE has been implicated in the pathophysiology of several neurodegenerative disorders including diabetic neuropathy (Petersen and Doorn 2004; Obrosova et al. 2005). Diabetic sensory neuropathy is one of the long-term clinical syndromes associated with poorly controlled diabetes mellitus (Said 2007; Yagihashi et al. 2007). Sensory nerves from human patients with neuropathy show progressive nerve fiber loss, endoneurial microangiopathy, and demyelination which often precedes axonal degeneration of myelinated fibers (Malik et al. 2005; Yagihashi et al. 2007). Key features of the disease are the targeting of lumbar dorsal root ganglia (DRG) sensory neurons with the longest axons and the distal loss of sensory nerve endings in the epidermis with subsequent failure to regenerate and/or undergo collateral sprouting (Lauria et al. 2003; Ebenezer et al. 2007). Complex metabolic pathways downstream of high glucose are involved in the etiology of this condition and include enhanced polyol pathway activity, increased nonenzymatic glycation of proteins, elevated oxidative stress, impaired neurotrophic support as well as changes in protein kinase C activity and/or MAP kinase activity (Brownlee 2001; Yagihashi et al. 2007; Calcutt et al. 2008; Tomlinson and Gardiner 2008). High [glucose]-induced generation of reactive oxygen species (ROS) by mitochondria has been proposed to link these mechanisms, suggesting a role for mitochondrial dysfunction and triggering of oxidative stress in the etiology of this disease (Brownlee 2001).

Increased levels of lipid peroxidation products, including 4-HNE and it's amino acid adducts, have been shown in the sciatic nerve and retina of streptozotocin (STZ)-diabetic rats, a model of type 1 diabetes (Obrosova et al. 2001; Obrosova et al. 2005), and also, modification of sorbitol dehydrogenase subunits has been associated with increased levels of 4-HNE in cardiomyopathy in diabetes (Lashin et al. 2006). Therefore, we hypothesized that increased levels of 4-HNE in diabetic tissues result in the formation of adducts on key mitochondrial and cytoskeletal proteins, this in-turn impairs mitochondrial activity and axonal function. The aim of this study was to expose cultured DRG sensory neurons from adult rats to 4-HNE and assess the presence of protein adducts of 4-HNE and their putative effect on mitochondrial function and axonal morphology and/or regeneration. In addition, our purpose was to compare effects of direct 4-HNE treatment of normal neurons with the phenotype of DRG cultures derived from STZ-diabetic rats.

Materials and Methods

Adult Rat and Mouse DRG Sensory Neuron Culture

DRG sensory neurons from adult male Sprague-Dawley rats or male Swiss Webster mice were isolated and dissociated using previously described methods (Huang et al. 2003; Gardiner et al. 2005; Huang et al. 2005a, b). Rats were either age-matched control or 3–4 month STZ-diabetic. Rats were made diabetic with a single i.p. injection of 75 mg/kg STZ (Sigma). Endpoints were as follows: body weight − control, 619.2 ± 47.6 g, diabetic, 360.9 ± 55.0 g; blood glucose − control, 9.14 ± 2.36 mM, diabetic, 29.6 ± 2.4 mM; glycated hemoglobin (% HbA1c) − control, 4.88 ± 0.4%, diabetic, 8.67 ± 0.74%. All values are means ± SD, $n = 11$, $P < 0.001$ for control vs diabetic. All animal protocols carefully followed Canadian Committee on Animal Care (CCAC) guidelines. Cells were plated onto poly-d-L-ornithine hydrobromide and laminin-coated multi-well plates (Nunclon Surface, Ottawa, ON) for neuronal survival and axon outgrowth studies and 25 mm glass cover slips (Electron Microscopy Sciences, Hatfield, PA, German glass #1) for immunocytochemistry and measurement of mitochondrial localization. Neurons were grown in defined Hams F-12 medium with modified Bottenstein and Sato's N2 medium (with no insulin) containing 0.1 mg/ml transferrin, 20 nM progesterone, 100 μM putrescine, 30 nM sodium selenite, 1 mg/ml BSA, and supplemented with neurotrophic factors (NTFs): 1 nM insulin, 1 ng/ml nerve growth factor (NGF), 10 ng/ml glial cell line-derived neurotrophic factor (GDNF), and 10 ng/ml neurotrophin-3 (NT-3) (all obtained from Sigma). For neuron survival and axon outgrowth studies cultured DRG neurons from adult rats or mice were treated with 4-HNE concentrations ranging from 1.0 to 10.0 μM and assessed at 24–48 h. Neuronal survival was quantified by established methods (Mattson et al. 1995; Fernyhough et al. 2005). Briefly, viable neurons were counted before experimental treatment and at time points following treatment. Neurons that died in the intervals between examination points were usually absent, and the viability of the remaining neurons was assessed by morphological criteria. Neurons with membranes and soma with a smooth round appearance were considered viable, whereas neurons with fragmented or distended membranes and vacuolated soma were considered nonviable. Six images were collected randomly from each well at 24 h of culture using a phase-contrast light microscope (Nikon Diaphot, phase contrast inverted microscope) fitted with a 20× objective and equipped with camera (Nikon Coolpix 5000). Survival counts were confirmed using trypan blue staining. For neurite outgrowth measurements, images of cultures were collected from six randomly selected fields from each well using a phase-contrast light

microscope. The total number of neurons and number of intersects of their neurites with a vertical Weibel grid were counted using a morphometric approach and using Sigma-Scan Microsoft software as previously described (Gardiner et al. 2005). The number of intersects per neuron was taken as the measure of total axon outgrowth.

Immunocytochemistry for Detection of Protein Adducts of 4-HNE

Adult DRG neurons grown on glass cover slips were fixed with 4% paraformaldehyde in phosphate buffered saline (PBS, pH 7.4) for 15 min at room temperature and then permeabilized with 0.3% Triton X-100 in PBS for 5 min. Nonspecific binding was reduced by incubation for 1 h at room temperature in blocking buffer prepared from blocking reagent (Roche, Indianapolis, IN, Cat # 1 096 176) which was diluted with FBS and 1.0 mM PBS in proportion 3:1:1 for 1 h and washed with PBS three times. Fixed cells were then incubated with antibodies to β-tubulin isotype III (neuron specific; Sigma, Oakville, ON, 1:1000), (E)-4-hydroxy-2-nonenal adducts (anti-4-HNE adducts PAb (Alexis Biochemicals, San Diego, CA, 1:500) and phosphorylated neurofilament H (NFH) (neuron specific; SMI-31; Covance, Berkeley, CA, 1:500). DRG cultures were incubated overnight with primary antibody in a humidified chamber followed by FITC- and CY3-conjugated secondary antibodies (Jackson ImmunoResearch Laboratories, West Grove, PA, 1: 250) for 3 h at room temperature. Fluorescence signal was examined using a Carl Zeiss Axioscop-2 mot microscope with AxioVision 3 software and equipped with FITC, CY3, DAPI filters, and AxioCam camera.

Fluorescence Video Microscopy of Mitochondria in Live Cultures

For localization of actively respiring mitochondria live cultures were stained for 15 min with 1 μM chloromethyl-x-rosamine (CMXRos) dye (Molecular Probes, Eugene, OR) before being fixed for immunostaining for adducts of 4-HNE. For localization of total mitochondria DRG cultures were stained with 200 nM Mitotracker green dye (Molecular Probes, Eugene, OR) for 15 min followed by 1 μM CMX-Ros. The fluorescence signal was examined using a Carl Zeiss LSM510 confocal inverted microscope in all experiments (care was taken to minimize excitation of the dyes given their propensity to generate free radical damage).

Quantification of Fluorescence Signals in Axons

Fluorescence signals along the axons in each field of view were assessed using software described above. For the assessment of 4-HNE and phosphorylated neurofilament levels in Figs. 2g, h and 3h, a line of specific width was traced along the axons and the average line pixel intensity over a distance of 150 μm measured. To assess CMXRos, Mitotracker green, and 4-HNE levels in Figs. 5g, h and 6g, h, a line of specific width was traced along each axon and the pixel intensity per micrometer of axonal length measured.

Mitochondrial Isolation

Adult rat DRG were homogenized in mitochondria isolation buffer containing: 10 mM HEPES (pH 7.4), 200 mM mannitol, 70 mM sucrose, and 1 mM EGTA. The DRG homogenate was centrifuged at $800\times g$ for 10 min at 4°C followed by centrifugation of the supernatant at $8000\times g$ for 15 min. The pellets (mitochondrial enriched fraction) were then resuspended in mitochondrial isolation buffer.

Measurement of Levels of Protein Adducts of 4-HNE Using Western Blot

Cultured DRG neurons were harvested at 24 h following 4-HNE treatment into ice-cold neurofilament stabilization buffer containing: 0.1 M Pipes, 5 mM $MgCl_2$, 5 mM EGTA, 0.5% Triton X-100, 20% glycerol, 10 mM NaF, 1 mM PMSF, and protease inhibitor cocktail (Fernyhough et al. 1999). Proteins were assayed using DC protein assay (BioRad; Hercules, CA) and western blot analysis performed as previously described (Towbin et al. 1979; Wataya et al. 2002). The proteins from cultured DRG neurons (10 μg/lane) and isolated mitochondria (5 μg/lane) were resolved on an 8% and 12% SDS-PAGE gel respectively, and electroblotted (30 V, 16 h) onto a nitrocellulose membrane. Blots were then blocked in 5% nonfat milk containing 0.05% Tween overnight at 4°C, rinsed in phosphate buffered saline (pH 7.4) and then incubated with the primary antibody (anti-4-HNE adducts PAb; 1:1000) overnight at 4°C. Levels of total extracellular signal-regulated kinase (T-ERK; Covance, Berkeley, CA; 1:2000) were detected and used as a loading control (our previous work has shown no change in expression in diabetes and under a range of conditions in our cultures). After six washes of 10 min in PBS-Tween and PBS, secondary antibody was applied for 1 h at room temperature. The blots were rinsed, incubated in Super Signal West Pico (Pierce biotechnology, Rockford, IL), and imaged using the BioRad Fluor-S image analyzer.

Data Analysis

All data are presented as means ± SEM, unless stated otherwise. In Fig. 1, data were subjected to one-way ANOVA with post hoc comparison using the Dunnett one-sided test (SPSS vs 13 for Windows). In Fig. 7, data were subjected to two-way ANOVA with post hoc comparison

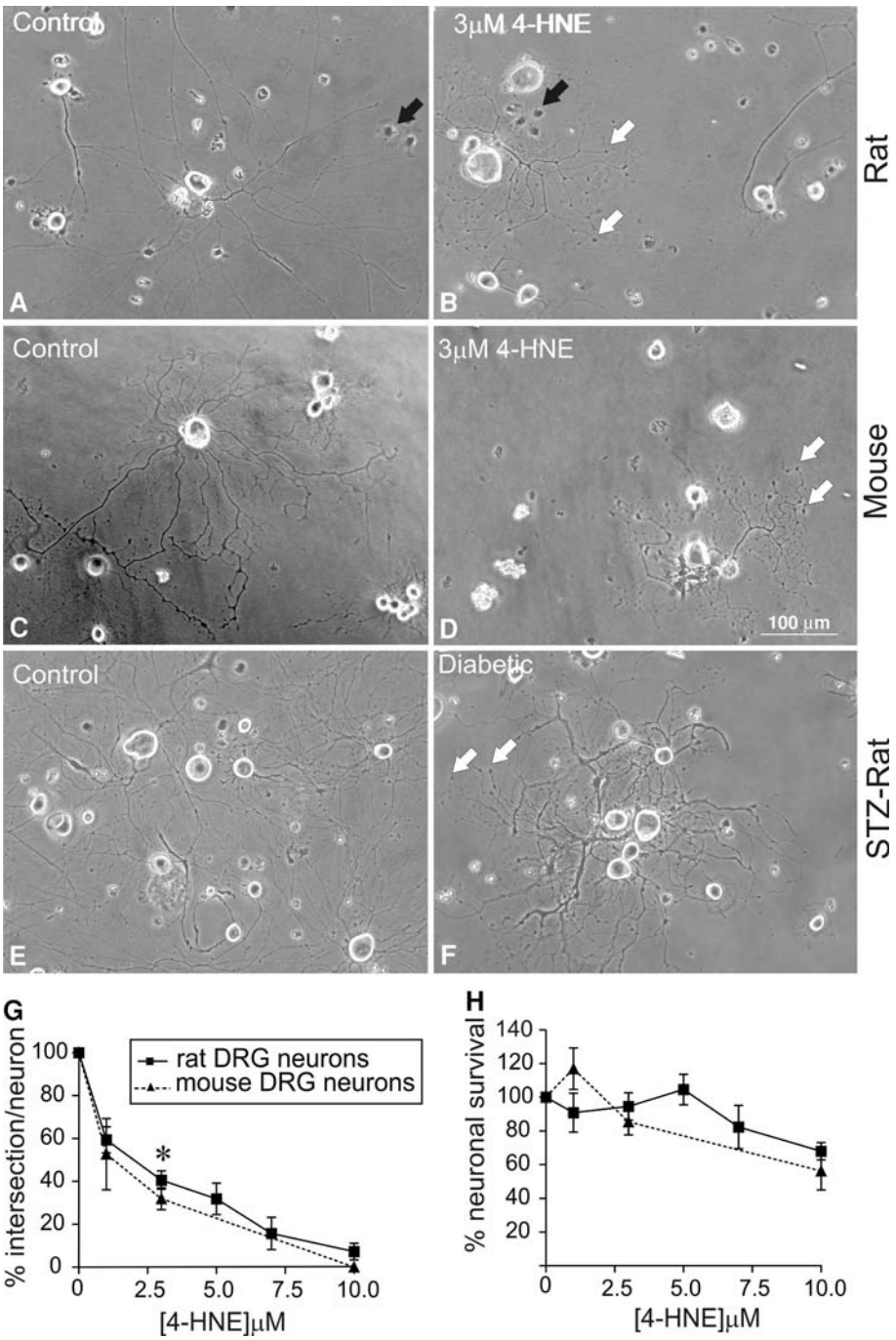

Fig. 1 Dose-dependent impairment of axonal outgrowth by 4-HNE. Figures **a** and **b** are phase contrast images of 24 h cultures of adult rat DRG sensory neurons. Figures **c** and **d** are images of 24 h cultures of adult mouse DRG sensory neurons. Neurons were grown in defined F12 media supplemented with N2 additives and neurotrophic factors (NTFs: 1 nM insulin, 1 ng/ml NGF, 10 ng/ml GDNF, and 10 ng/ml NT-3) and treated with 3.0 μM 4-HNE. Figures **e** and **f** are images of 3–4 day cultures of adult rat STZ diabetic neurons. Neurons were grown in defined F12 + N2 media supplemented with 10 mM glucose (control) and 25 mM glucose (diabetic). Figures **g** and **h** are the quantification of total axon outgrowth and levels of survival of DRG sensory neurons treated with 4-HNE ranging from 1.0 to 10 μM over a 24-h period. *White arrows* show swellings or dystrophic regions on the axons and *black arrows* show non-neurons. Values are means ± SEM, $n = 4$ replicate cultures. * $P < 0.05$ vs control in rat and mice

using Tukey's test. In all other cases, analysis was by standard two-tailed unpaired or paired Student *t*-test with significant levels of $P < 0.05$ using (GraphPad Prism 4, GraphPad Software Inc., San Diego, CA).

Results

Adult sensory neurons from normal adult rats (Fig. 1a, b) and mice (Fig. 1c, d) were cultured for 24 h in defined F12 + N2 medium supplemented with a cocktail of neurotrophic factors and treated with 4-HNE concentrations ranging from 1.0 to 10 μM. Cell survival, axon morphology, and level of axon outgrowth were assessed at 24 h of culture. 4-HNE significantly impaired axonal outgrowth by approximately 50% at a concentration of 2.5 μM in the rat sensory neuron culture (Fig. 1g) while having no effect on neuronal survival at this concentration. Thus, EC_{50} for the inhibition of neurite outgrowth by 4-HNE was found to be significantly lower than that for decreased neuronal survival (Fig. 1h). Impairment of axonal outgrowth in the rat culture was not significantly different from the mouse culture,

however, there was a slight shift of the mouse dose response curve to the left (Fig. 1g). 4-HNE-treated cultures also exhibited aberrant axonal structures with phase dark swellings or dystrophic structures along axons (Fig. 1b, d; white arrows) which were absent or minimal in control cultures (Fig. 1a, c). These effects of 4-HNE on axon outgrowth and morphology were compared with features of axon outgrowth produced by adult sensory neurons isolated from 3 to 4 month STZ-diabetic rats. Age-matched control and diabetic neurons were incubated in defined F12 + N2 medium with normal glucose (10 mM) and high glucose (25 mM), respectively, and assessed at 3–4 days of culture. The longer growth period was required to allow time for high glucose concentration-dependent oxidative stress to develop and permit adducts of 4-HNE to build up and induce pathology (Fig. 1f). The diabetic neurons revealed approximately 50% reduction in axon outgrowth (data not shown) and formation of phase dark swellings along axons (Fig. 1e, f) as observed under conditions of 4-HNE treatment in normal neurons.

The ability of 4-HNE to form amino acid adducts on cytoskeletal proteins in rat sensory neurons and as a result alter the phosphorylation of neurofilament proteins was investigated. Sensory neurons from normal rats were treated at 24 h of culture with 3 μM 4-HNE and immunostained (following 24 h of treatment) for phosphorylated NFH (Fig. 2a, b) and adducts of 4-HNE (Fig. 2c, d). Control cultures showed normal axons with minimal labeling of adducts of 4-HNE (Fig. 2c), whereas, 4-HNE-treated cultures showed large numbers of aggregations or puncta of 4-HNE staining (Fig. 2d; white arrows). Figure 2g shows a twofold increase in adduct formation compared to controls and Fig. 2h shows a significant increase in NFH phosphorylation in the treated group. Sensory neurons were also cultured for 4 days from age-matched control and 3–4 month STZ-diabetic rats and immunostained for β-tubulin III (Fig. 3a, b) and adducts of 4-HNE (Fig. 3c, d). The control group exhibited normal axons with minimal swellings, whereas, neurons from diabetic rats presented with axonal swellings, which stained positive for adducts of 4-HNE (Fig. 3d; white arrows). Figure 3g, h shows an increase in number of abnormal axonal swellings and total levels of adducts of 4-HNE in the axons of diabetic neurons, respectively.

Normal sensory neurons were treated with 4-HNE for 24 h of culture. The cell lysates were harvested and protein adducts of 4-HNE assessed by western blotting (Fig. 4a). There was a clear enhancement in adduct formation in the 4-HNE-treated group, with discernable bands showing up around 25, 55, 70, 130 KDa. These molecular weights are similar to those of cytochrome C oxidase, ATPase synthase, neurofilament L, and neurofilament M, respectively. Also, mitochondria were isolated from normal and STZ-diabetic adult rat DRG and protein adducts of 4-HNE assessed by

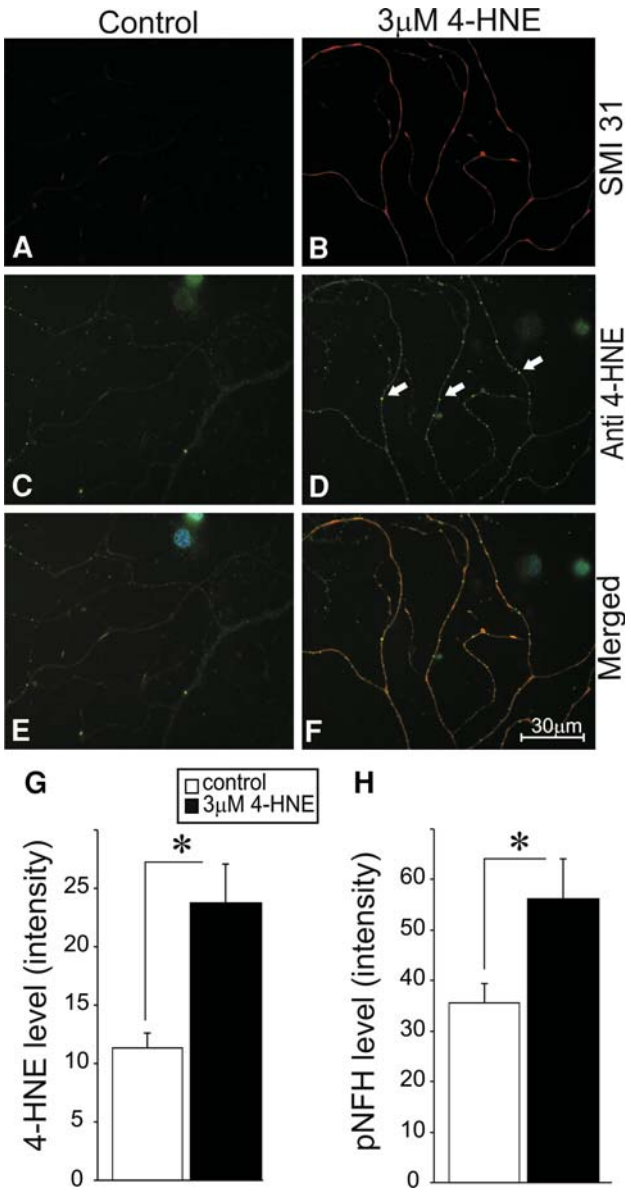

Fig. 2 4-HNE-treated adult rat DRG neurons exhibit aberrant axonal structures containing adducts of 4-HNE. Figures **a** and **b** were stained for phosphorylated NFH using antibody SMI 31 (*red*). Figures **c** and **d** are stained for adducts of 4-HNE using anti-HNE polyclonal antibody (anti-HNE PAb; *green*). Figures **e** and **f** are merged images of adducts of 4-HNE and phosphorylated NFH (blue nuclei stained with DAPI). Neurons were grown in defined F12 media supplemented with N2 additives and neurotrophic factors and treated with 3.0 μM 4-HNE. *White arrows* show accumulation of 4-HNE adducts. Figures **g** and **h** are the quantification of levels of protein adducts and phosphorylated NFH in the axons, respectively. Values are means ± SEM, $n = 45$ axons. * $P < 0.05$ (color figure online)

western blot (Fig. 4b). There was an increase in adduct formation in the STZ diabetic rat DRG at molecular weights corresponding to 15 KDa (Fig. 4c) and 40 KDa (Fig. 4b). The combined intensity of all the discernable bands on the blot (Fig. 4b) showed an increase in adduct formation in the STZ diabetic rat DRG compared to the controls (Fig. 4f).

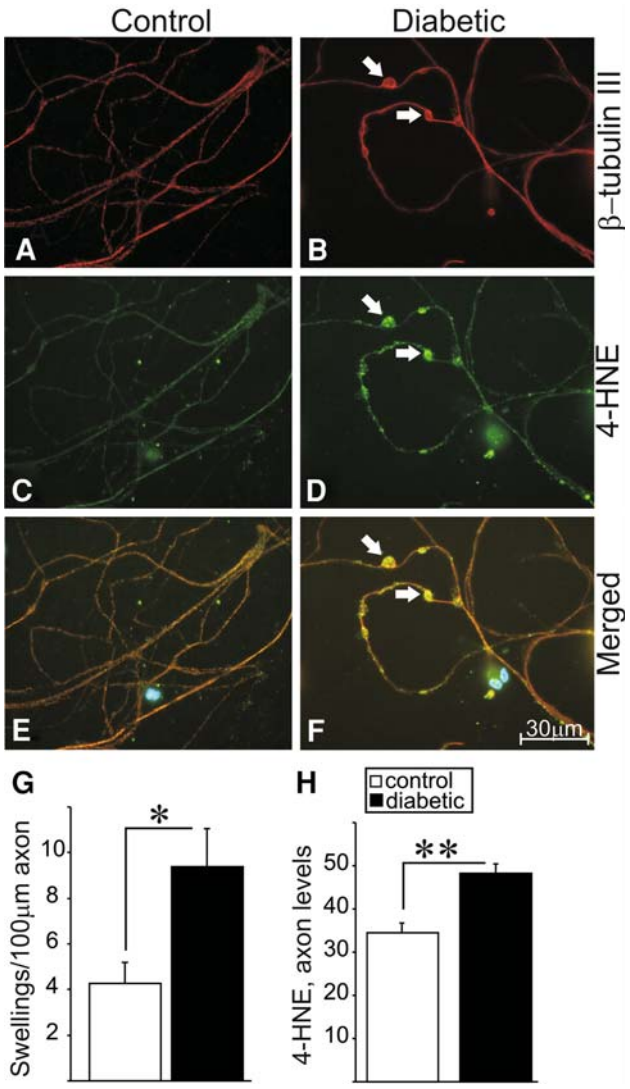

Fig. 3 Axons of neurons of STZ-diabetic rats exhibit swellings that express adducts of 4-HNE. Figures **a**, **c**, and **e** represent immunofluorescent images derived from lumbar DRG sensory neurons cultured from age-matched control rats. Cells were grown for 4 days in F12 + N2 defined medium with 10 mM D-glucose and with 10 nM insulin. Figures **b**, **d**, and **f** represent immunofluorescent images derived from lumbar DRG sensory neurons cultured from 3- to 4-month STZ-diabetic rats grown in F12 + N2 defined medium with 25 mM D-glucose and without insulin. Figures **a** and **b** represent staining for neuron-specific *β*-tubulin III (*red*), **c** and **d** is staining for adducts of 4-HNE, and **e** and **f** are merged images (blue nuclei stained with DAPI). Figures **g** and **h** are quantification of number of swellings per 100 μm of axon length and 4-HNE level in axons. Values are means ± SEM, $n = 3$ replicates. * $P < 0.05$, ** $P < 0.001$ (color figure online)

Mitochondrial function has a central role in governing axon outgrowth, mainly through generation of ATP for actin treadmilling (Bernstein and Bamburg 2003), and so the effect of 4-HNE adduct formation on the activity of mitochondria was analyzed in normal adult rat sensory neuron cultures. Sensory neurons were treated with 3 μM 4-HNE at 24 h and co-stained for actively respiring mitochondria using CMXRos (Fig. 5a, b) (following 24 h of treatment) and adducts of 4-HNE (Fig. 5c, d). CMXRos dye produces low fluorescence until entry into an actively respiring cell, where it becomes oxidized to the fluorescent mitochondrion selective-probe and then covalently sequestered in the mitochondria—the level of entry into the mitochondrion is dependent upon the extent of mitochondrial depolarization and hence, in part, directly related to mitochondrial respiratory activity; the more polarized the mitochondrial inner membrane the greater the uptake of dye. Control cultures exhibited normal axons with uniform labeling of actively respiring mitochondria and minimal swellings (Fig. 5a) which stained negatively for adducts of 4-HNE (Fig. 5c). In comparison, 4-HNE-treated cultures showed much less uniform staining for active mitochondria with a large number of axonal swellings that were filled with active mitochondria (Fig. 5b) and which stained positively for adducts of 4-HNE (Fig. 5d). The accumulation of adducts of 4-HNE co-located with active mitochondria in the axonal swellings (Fig. 5f; white arrows). Increase in the formation of 4-HNE adducts in the axons (Fig. 5h) after 4-HNE treatment was associated with a decrease in the levels of active mitochondria as indicated by CMXRos intensity levels (Fig. 5g). We next investigated if a decline in actively respiring mitochondrial levels resulted in a reduction in mitochondrial mass (active and inactive) in sensory neurons treated with 4-HNE. Sensory neurons were treated with 3 μM 4-HNE at 24 h and co-stained with Mitotracker green dye (Fig. 6a, b) and CMXRos (Fig. 6c, d) (following 24 h of treatment). Mitotracker green dye preferentially accumulates in mitochondria regardless of mitochondrial membrane potential, making it a tool for determining mitochondria mass. Mitochondria mass as indicated by Mitotracker green intensity was evenly spread from the cell body to the axon terminals in the absence or presence of 4-HNE (Fig. 6a, b), however, a progressive decline in CMXRos signal intensity was observed toward the distal axonal regions in the 4-HNE-treated group (Fig. 6c, d). There was no statistical difference between the treated and control groups with respect to Mitotracker green levels in the axons (Fig. 6g); however, CMXRos intensity levels declined significantly in the treated group compared to control (Fig. 6h). The pattern of expression of active mitochondrial levels was studied in normal sensory neurons treated with 4-HNE over a time course of 24 h. Sensory neurons were treated with 3 μM 4-HNE at 24 h and stained with CMXRos at 12, 18, and 24 h of treatment (Fig. 7). There was a significant 4-HNE-induced decrease in the levels of active mitochondria at 12 and 18 h compared to controls, however, mitochondrial activity levels began to recover at 24 h even though the levels at this time point were still significantly lower than controls.

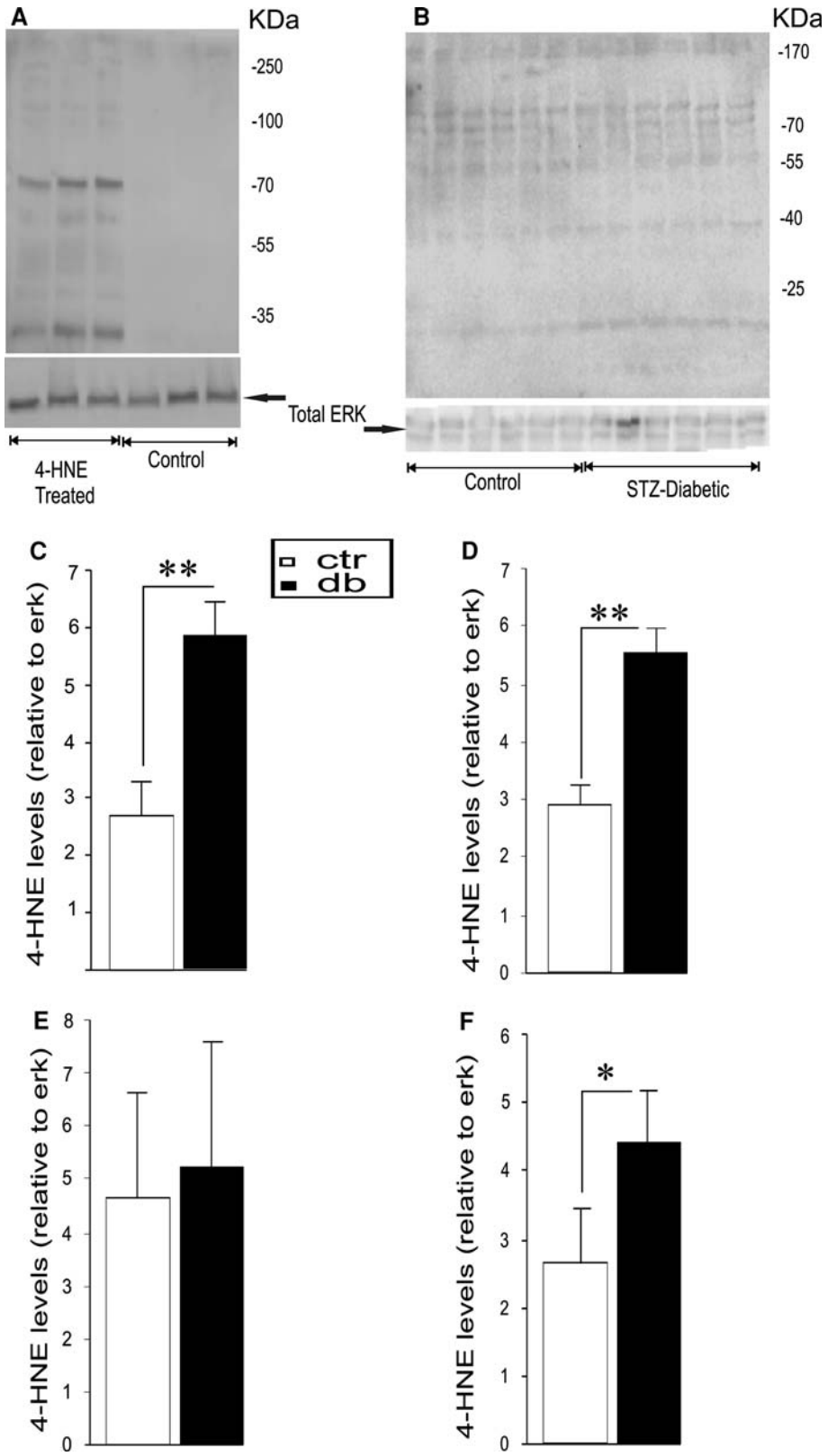

Fig. 4 4-HNE adduct formation in cultures of adult DRG and in DRG mitochondrial preparations from STZ-diabetic rats. **a** Western blot showing protein adducts formation in cultured neurons using anti-HNE antibody. Neurons were grown in defined F12 media supplemented with modified N2 additives and neurotrophic factors (NTFs; 1 nM insulin, 1 ng/ml NGF, 10 ng/ml GDNF and 10 ng/ml NT-3) and treated with 3.0 μM 4-HNE for 24 h. **b** Western blot showing protein adducts formation in mitochondria from DRG of normal or STZ-diabetic rats. Mitochondria were isolated from DRG of adult STZ-diabetic and normal rats using mitochondria isolation buffer containing: 10 mM HEPES (pH 7.4), 200 mM mannitol, 70 mM sucrose, and 1 mM EGTA. Figures **c–e** are the quantifications of the levels of protein adducts relative to total ERK on blot (**b**) at 15, 40, and 170 KDa, respectively. Figure **f** is a quantification of total levels of protein adducts on blot (**b**) in normal and STZ-diabetic DRG mitochondria. The band intensities from all the discernable bands on blot (**b**) were pooled together to generate (**f**). Values are means ± SEM, $n = 6$ replicates. $^{*}P < 0.05$, $^{**}P < 0.001$

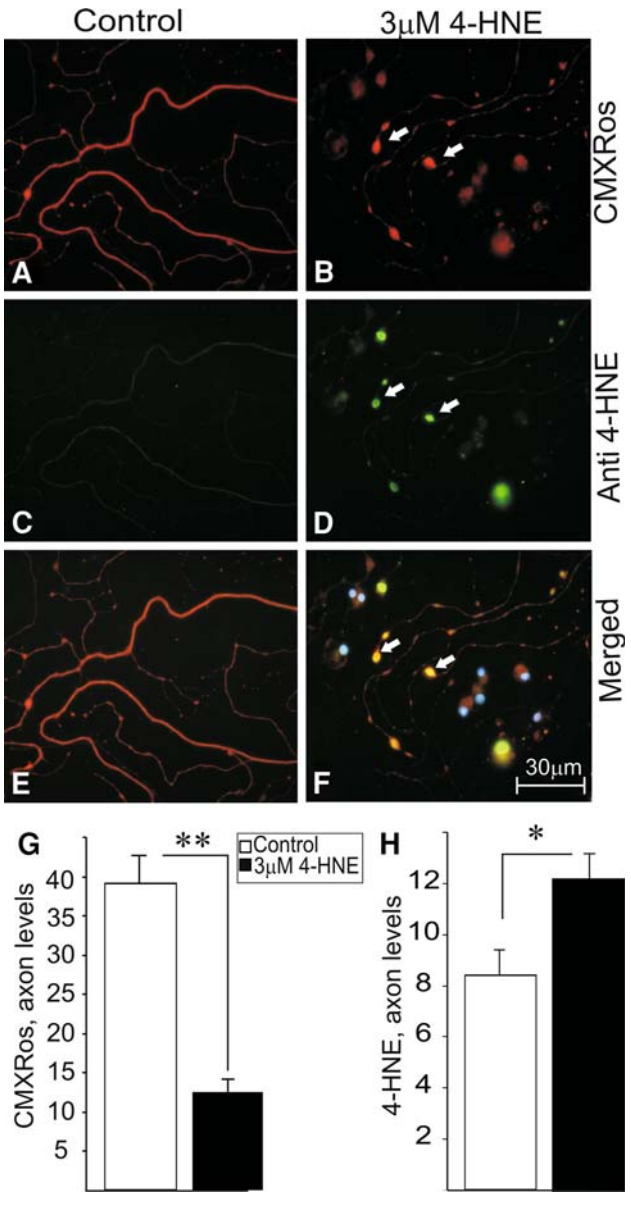

Fig. 5 4-HNE induces the accumulation of active mitochondria in swellings along the axons of adult rat DRG neurons. Figures **a** and **b** are stained for active mitochondria (*red*) using chloromethyl-x-rosamine (CMXRos). Figures **c** and **d** show the presence of adducts of 4-HNE using anti-HNE PAb. **e** and **f** represent merged images of adducts of 4-HNE and active mitochondria (blue nuclei stained with DAPI). Neurons were grown in defined F12 media supplemented with N2 additives and neurotrophic factors and treated with 3.0 μM 4-HNE. *Note*: neurons were treated with 4-HNE at 24 h of neuronal culture and immunofluorescence images taken at 24 h of treatment. White arrows indicate the presence of axonal swellings. Figures **g** and **h** are the quantification of active mitochondria and adducts of 4-HNE levels in the axons, respectively. Values are means ± SEM, $n = 48$ axons. * $P < 0.05$ and ** $P < 0.01$ (color figure online)

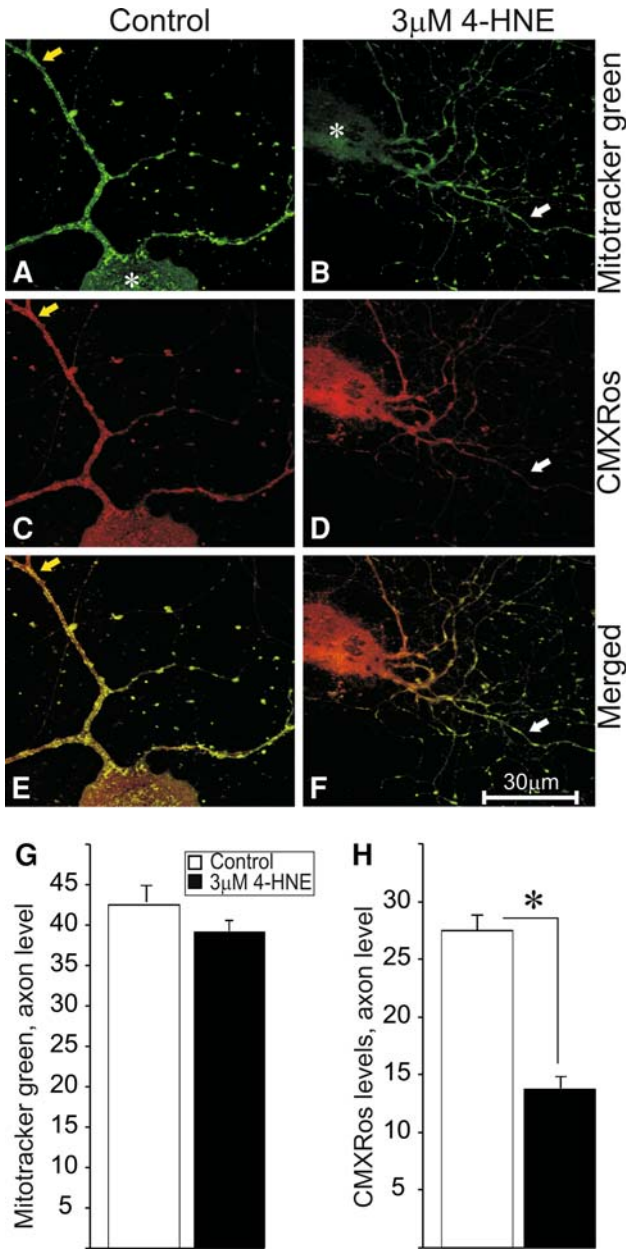

Fig. 6 Reduction in levels of active mitochondria in the axons of 4-HNE-treated adult rat DRG neurons. Figures **a** and **b** are stained for total mitochondria using Mitotracker green dye. Figures **c** and **d** are stained for active mitochondria (*red*) using CMXRos. Neurons were grown in defined F12 media supplemented with N2 additives and neurotrophic factors and treated with 3.0 μM 4-HNE. *Note*: neurons were treated with 4-HNE for 24 h following 24 h of neuronal culture. Figures **e** and **f** are merged images. Figures **g** and **f** are the quantification of total and active mitochondria level in the axons, respectively. *White arrows* indicate area of relative loss of active mitochondria. The asterisk shows cell body of neurons. Values are means ± SEM, $n = 48$ axons. * $P < 0.05$ (color figure online)

Discussion

There is increasing evidence of the role played by oxidative damage including lipid peroxidation in the etiology of a range of neurodegenerative diseases, including development of diabetic neuropathy (Neely et al. 1999; Obrosova et al. 2005). 4-HNE, a product of lipid peroxidation, forms adducts with key neuronal proteins (Uchida 2003; Petersen

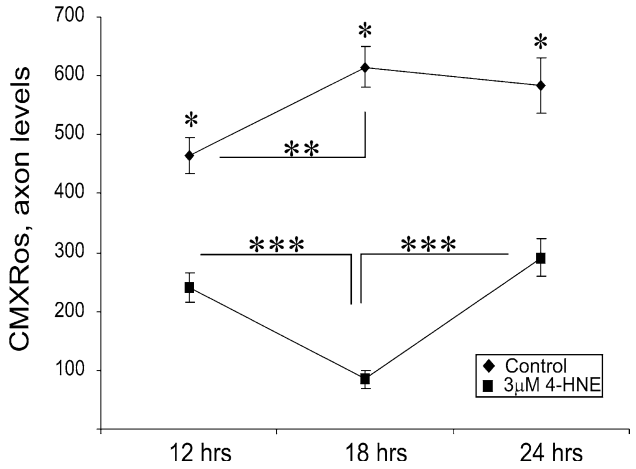

Fig. 7 Expression of active mitochondria in 4-HNE-treated adult rat DRG neurons. Graph showing the levels of active mitochondria over a period of 24 h. Neurons were grown in defined F12 media supplemented with N2 additives and neurotrophic factors and treated with 3.0 μM 4-HNE. *Note*: neurons were treated with 4-HNE at 24 h. Values are means ± SEM, $n = 48$ axons. * $P < 0.05$, ** $P < 0.01$, and *** $P < 0.001$

and Doorn 2004), and these adducts have been shown to be elevated in the peripheral nerves of STZ-diabetic rats (Obrosova et al. 2005). Protein adducts have also been detected in mouse sciatic nerves treated with 4-HNE (Wataya et al. 2002) and sciatic nerves and DRG of diabetic mice exposed to a high fat diet (a model of pre-diabetes) (Obrosova et al. 2007). In the present study we show for the first time that 4-HNE directly impairs mitochondrial function and axonal regeneration in cultured adult DRG sensory neurons. 4-HNE triggered formation of amino acid adducts of neuronal proteins, including mitochondrial proteins, and this was associated with a distally directed reduction in the levels of active mitochondria in the axon, and the formation of abnormal axonal structures, which stained positively for adducts of 4-HNE. These structural abnormalities in the axons closely resembled dystrophic and 4-HNE-labeled structures observed in the neurites of DRG neuronal cultures derived from STZ-diabetic rats (Fig. 3). Our results, with regards to the ability of 4-HNE to form adducts on neuronal proteins and impair mitochondrial activity, are in good agreement with studies on other types of cells. For example, studies by the Romani group showed specific modification of key mitochondrial proteins by 4-HNE leading to an impairment in enzymatic activity in the mitochondria of cardiac tissue in rodents with diabetes (Lashin et al. 2006).

The axonal pathology induced by 4-HNE in the normal cultures closely paralleled axon damage generated in cultures of neurons from diabetic rats. Interestingly, the anatomical phenotype of these cultures described herein exhibited axonal morphologies that closely compare with axon pathology in human diabetic neuropathy where axonal swellings and dystrophy have been described in DRG, nerve and at distal sites within the epidermis (Schmidt et al. 1997; Lauria et al. 2003; Ebenezer et al. 2007). In diabetes, it has been proposed that axonal pathology may be triggered by impaired mitochondrial function (Sasaki et al. 1997; Brownlee 2001; Fernyhough et al. 2003; Verkhratsky and Fernyhough 2008). It has been theorized that high [glucose] drives excessive electron donation to the electron transport chain in mitochondria resulting in mitochondrial hyperpolarization and elevated production of ROS (Nishikawa et al. 2000). Brownlee et al. have proposed that this mitochondrial-dependent process is a central mediator of oxidative stress in complications of diabetes and could be a major generator of lipid peroxidation and 4-HNE (Brownlee 2001). The theory suggests that high [glucose] in tissue targets for diabetic complications leads to increased supply of NADH in the mitochondria, and that this increased electron availability and/or saturation may cause partial reduction of oxygen to superoxide radicals in the proximal part of the electron transport chain. Subsequent large elevations in ROS and associated 4-HNE then may react with mitochondrial proteins and result in degeneration of tissue. These findings point to the central role played by the mitochondria, and in part 4-HNE, as a mediator of neurodegeneration in the PNS and a critical modulator of diabetic complications in neurons (Sasaki et al. 1997; Brownlee 2001; Fernyhough et al. 2003; Verkhratsky and Fernyhough 2008).

The current study revealed that 4-HNE formed adducts and significantly impaired neurite outgrowth at concentrations as low as 3 μM in cultured adult DRG neurons treated with 4-HNE for a period of 24 h. Also, significant neuronal death was observed at 4-HNE concentrations of 10 μM or higher in the DRG cultures. Other studies have reported impairment of neurite outgrowth in Neuro 2A cells incubated with 4-HNE for 1 h and assessment of outgrowth made 24 h later (Neely et al. 1999). The former study showed no significant impairment of neurite outgrowth at 4-HNE concentrations below 25 μM, and found no significant cell death. These discrepancies could be the result of differences in cell types, period of 4-HNE exposure and extent of cell density (Kokubo et al. 2008). For example, within the present study there was enhanced sensitivity of the mouse DRG neuronal cultures to 4-HNE. It is worth noting that one of the key pathological features of diabetic neuropathy as observed in humans and in animal models involves the dying back of the longest axons, however, these neurons do not undergo any overt process of cell death (Schmidt et al. 1997). Therefore, in our cultured DRG neurons, we determined the concentration of 4-HNE at which there was approximately 50% impairment in neurite outgrowth with no corresponding effect on neuronal survival. 4-HNE concentration of 2.5 μM appeared to be

the ideal dose; however, we adjusted this to 3.0 μM taking into account the slight variability in neuronal numbers from different cultures.

The important finding in the present study was that 4-HNE was associated with a distally directed reduction in the levels of actively respiring mitochondria, and with the formation of swellings along the axons, further implicating the role of mitochondrial dysfunction in the etiology of the axon pathology. Also, the fact that the protein adducts of 4-HNE co-localized with actively respiring mitochondria in areas of swellings along the axons points to the fact that some mitochondrial proteins might have been modified. This result, with regard to the localization of mitochondria to sites of swellings along the axon, agrees with in vitro studies by the Connolly group (Greenwood et al. 2007). Western blot analysis of mitochondria isolated from adult STZ-diabetic and normal rats indicate that one of the target proteins for 4-HNE adduction might be cytochrome C oxidase (Complex IV enzyme), although, other targets such as succinate dehydrogenase have been reported (Lashin et al. 2006). Also, studies concerning adduction of 4-HNE to proteins have demonstrated its ability to inhibit a variety of enzymes including complex IV of the mitochondrial respiratory chain (Isom et al. 2004). Cytochrome C is essential for the translocation of electrons between Complex III and IV, a key process that generates the proton gradient that drives ATP synthase activity (Complex V) (Nicholls and Ward 2000). Modification of this key enzyme in the electron transport chain could result in diminished ATP production. A reduction in ATP synthesis in the axon from either disruption in proton gradient generation or improper mitochondrial localization could lead to decreased Na^+–K^+ ATPase function, resulting in a rise in intracellular Na^+ and a reversal of Na^+–Ca^{2+} exchanger function (Waxman 2006). The outcome could be an increase in intracellular Ca^{2+} to damaging levels, ultimately resulting in axonal degeneration (Duchen et al. 2008; Verkhratsky and Fernyhough 2008). It should be noted that abnormal Ca^{2+} homeostasis is also a key feature of sensory neuron dysfunction in animal models of type 1 and type 2 diabetes (Huang et al. 2002; Verkhratsky and Fernyhough 2008). Moreover, we believe the presence of axonal swellings mediated by an accumulation of modified mitochondria and/or aberrantly phosphorylated neurofilament proteins could physically obstruct the movement of mitochondria toward the axonal terminals. Disruption of proper mitochondrial motility and localization is believed to interfere with normal axonal and synaptic function and could likely result in distal axonal degeneration (Baloh 2008).

In conclusion, we propose that increased intracellular levels of 4-HNE leads to the modification of key mitochondrial proteins through adduct formation, this causes a disruption in the activity and localization of mitochondria and could trigger an impaired bioenergetic state within axons, eventually leading to axonal degeneration. The axonal degeneration induced by 4-HNE closely resembles aberrant axon morphology observed in neurons from a diabetic background, a key feature in both settings is the presence of 4-HNE-labeled axonal swellings. In summary, these results implicate lipid peroxidation and 4-HNE adduct formation, possibly targeted to the mitochondrion, in the neurodegenerative processes central to the etiology of diabetic sensory neuropathy.

Acknowledgments This work was supported by grants to PF from CIHR (Grants # ROP-72893 and MOP-84214), Juvenile Diabetes Research Foundation (Grant # 1-2008-193), NSERC (Grant # 311686-06), and St Boniface General Hospital and Research Foundation.

References

Awasthi YC, Sharma R, Cheng JZ, Yang Y, Sharma A, Singhal SS, Awasthi S (2003) Role of 4-hydroxynonenal in stress-mediated apoptosis signaling. Mol Aspects Med 24:219–230

Baloh RH (2008) Mitochondrial dynamics and peripheral neuropathy. Neuroscientist 14:12–18

Bernstein BW, Bamburg JR (2003) Actin-ATP hydrolysis is a major energy drain for neurons. J Neurosci 23:1–6

Brownlee M (2001) Biochemistry and molecular cell biology of diabetic complications. Nature 414:813–820

Calcutt NA, Jolivalt CG, Fernyhough P (2008) Growth factors as therapeutics for diabetic neuropathy. Curr Drug Target 9:47–59

Carini M, Aldini G, Facino RM (2004) Mass spectrometry for detection of 4-hydroxy-trans-2-nonenal (HNE) adducts with peptides and proteins. Mass Spectrom Rev 23:281–305

Duchen MR, Verkhratsky A, Muallem S (2008) Mitochondria and calcium in health and disease. Cell Calcium 44:1–5

Ebenezer GJ, McArthur JC, Thomas D, Murinson B, Hauer P, Polydefkis M, Griffin JW (2007) Denervation of skin in neuropathies: the sequence of axonal and Schwann cell changes in skin biopsies. Brain 130:2703–2714

Fernyhough P, Gallagher A, Averill SA, Priestley JV, Hounsom L, Patel J, Tomlinson DR (1999) Aberrant neurofilament phosphorylation in sensory neurons of rats with diabetic neuropathy. Diabetes 48:881–889

Fernyhough P, Huang TJ, Verkhratsky A (2003) Mechanism of mitochondrial dysfunction in diabetic sensory neuropathy. J Peripher Nerv Syst 8:227–235

Fernyhough P, Smith DR, Schapansky J, Van Der Ploeg R, Gardiner NJ, Tweed CW, Kontos A, Freeman L, Purves-Tyson TD, Glazner GW (2005) Activation of nuclear factor-kappaB via endogenous tumor necrosis factor alpha regulates survival of axotomized adult sensory neurons. J Neurosci 25:1682–1690

Forman HJ, Dickinson DA, Iles KE (2003) HNE-signaling pathways leading to its elimination. Mol Aspects Med 24:189–194

Gardiner NJ, Fernyhough P, Tomlinson DR, Mayer U, von der Mark H, Streuli CH (2005) Alpha7 integrin mediates neurite outgrowth of distinct populations of adult sensory neurons. Mol Cell Neurosci 28:229–240

Greenwood SM, Mizielinska SM, Frenguelli BG, Harvey J, Connolly CN (2007) Mitochondrial dysfunction and dendritic beading during neuronal toxicity. J Biol Chem 282:26235–26244

Huang TJ, Sayers NM, Fernyhough P, Verkhratsky A (2002) Diabetes-induced alterations in calcium homeostasis in sensory neurones of streptozotocin-diabetic rats are restricted to lumbar

ganglia and are prevented by neurotrophin-3. Diabetologia 45:560–570

Huang TJ, Price SA, Chilton L, Calcutt NA, Tomlinson DR, Verkhratsky A, Fernyhough P (2003) Insulin prevents depolarization of the mitochondrial inner membrane in sensory neurons of type 1 diabetic rats in the presence of sustained hyperglycemia. Diabetes 52:2129–2136

Huang TJ, Verkhratsky A, Fernyhough P (2005a) Insulin enhances mitochondrial inner membrane potential and increases ATP levels through phosphoinositide 3-kinase in adult sensory neurons. Mol Cell Neurosci 28:42–54

Huang TJ, Sayers NM, Verkhratsky A, Fernyhough P (2005b) Neurotrophin-3 prevents mitochondrial dysfunction in sensory neurons of streptozotocin-diabetic rats. Exp Neurol 194:279–283

Isom AL, Barnes S, Wilson L, Kirk M, Coward L, Darley-Usmar V (2004) Modification of Cytochrome c by 4-hydroxy-2-nonenal: evidence for histidine, lysine, and arginine-aldehyde adducts. J Am Soc Mass Spectrom 15:1136–1147

Karlhuber GM, Bauer HC, Eckl PM (1997) Cytotoxic and genotoxic effects of 4-hydroxynonenal in cerebral endothelial cells. Mutat Res 381:209–216

Kokubo J, Nagatani N, Hiroki K, Kuroiwa K, Watanabe N, Arai T (2008) Mechanism of destruction of microtubule structures by 4-hydroxy-2-nonenal. Cell Struct Funct 33:51–59

Lashin OM, Szweda PA, Szweda LI, Romani AM (2006) Decreased complex II respiration and HNE-modified SDH subunit in diabetic heart. Free Radic Biol Med 40:886–896

Lauria G, Morbin M, Lombardi R, Borgna M, Mazzoleni G, Sghirlanzoni A, Pareyson D (2003) Axonal swellings predict the degeneration of epidermal nerve fibers in painful neuropathies. Neurology 61:631–636

Malik RA, Tesfaye S, Newrick PG, Walker D, Rajbhandari SM, Siddique I, Sharma AK, Boulton AJ, King RH, Thomas PK, Ward JD (2005) Sural nerve pathology in diabetic patients with minimal but progressive neuropathy. Diabetologia 48:578–585

Mattson MP, Barger SW, Begley JG, Mark RJ (1995) Calcium, free radicals, and excitotoxic neuronal death in primary cell culture. Methods Cell Biol 46:187–216

Neely MD, Sidell KR, Graham DG, Montine TJ (1999) The lipid peroxidation product 4-hydroxynonenal inhibits neurite outgrowth, disrupts neuronal microtubules, and modifies cellular tubulin. J Neurochem 72:2323–2333

Nicholls DG, Ward MW (2000) Mitochondrial membrane potential and neuronal glutamate excitotoxicity: mortality and millivolts. Trends Neurosci 23:166–174

Nishikawa T, Edelstein D, Du XL, Yamagishi S, Matsumura T, Kaneda Y, Yorek MA, Beebe D, Oates PJ, Hammes HP, Giardino I, Brownlee M (2000) Normalizing mitochondrial superoxide production blocks three pathways of hyperglycaemic damage. Nature 404:787–790

Obrosova IG, Minchenko AG, Marinescu V, Fathallah L, Kennedy A, Stockert CM, Frank RN, Stevens MJ (2001) Antioxidants attenuate early up regulation of retinal vascular endothelial growth factor in streptozotocin-diabetic rats. Diabetologia 44:1102–1110

Obrosova IG, Drel VR, Pacher P, Ilnytska O, Wang ZQ, Stevens MJ, Yorek MA (2005) Oxidative-nitrosative stress and poly(ADP-ribose) polymerase (PARP) activation in experimental diabetic neuropathy: the relation is revisited. Diabetes 54:3435–3441

Obrosova IG, Ilnytska O, Lyzogubov VV, Pavlov IA, Mashtalir N, Nadler JL, Drel VR (2007) High-fat diet induced neuropathy of pre-diabetes and obesity: effects of "healthy" diet and aldose reductase inhibition. Diabetes 56:2598–2608

Petersen DR, Doorn JA (2004) Reactions of 4-hydroxynonenal with proteins and cellular targets. Free Radic Biol Med 37:937–945

Said G (2007) Diabetic neuropathy—a review. Nat Clin Pract Neurol 3:331–340

Sasaki H, Schmelzer JD, Zollman PJ, Low PA (1997) Neuropathology and blood flow of nerve, spinal roots and dorsal root ganglia in longstanding diabetic rats. Acta Neuropathol 93:118–128

Sayre LM, Lin D, Yuan Q, Zhu X, Tang X (2006) Protein adducts generated from products of lipid oxidation: focus on HNE and one. Drug Metab Rev 38:651–675

Schmidt RE, Dorsey D, Parvin CA, Beaudet LN, Plurad SB, Roth KA (1997) Dystrophic axonal swellings develop as a function of age and diabetes in human dorsal root ganglia. J Neuropathol Exp Neurol 56:1028–1043

Tomlinson DR, Gardiner NJ (2008) Glucose neurotoxicity. Nat Rev Neurosci 9:36–45

Towbin H, Staehelin T, Gordon J (1979) Electrophoretic transfer of proteins from polyacrylamide gels to nitrocellulose sheets: procedure and some applications. Proc Natl Acad Sci U S A 76:4350–4354

Uchida K (2003) 4-Hydroxy-2-nonenal: a product and mediator of oxidative stress. Prog Lipid Res 42:318–343

Verkhratsky A, Fernyhough P (2008) Mitochondrial malfunction and Ca^{2+} dyshomeostasis drive neuronal pathology in diabetes. Cell Calcium 44:112–122

Wataya T, Nunomura A, Smith MA, Siedlak SL, Harris PL, Shimohama S, Szweda LI, Kaminski MA, Avila J, Price DL, Cleveland DW, Sayre LM, Perry G (2002) High molecular weight neurofilament proteins are physiological substrates of adduction by the lipid peroxidation product hydroxynonenal. J Biol Chem 277:4644–4648

Waxman SG (2006) Ions, energy and axonal injury: towards a molecular neurology of multiple sclerosis. Trends Mol Med 12:192–195

Yagihashi S, Yamagishi S, Wada R (2007) Pathology and pathogenetic mechanisms of diabetic neuropathy: correlation with clinical signs and symptoms. Diabetes Res Clin Pract 77(Suppl 1): S184–S189